Supporting online materials for

Ultrahigh compressibility and superior elasticity carbon framework derived from shaddock peel for high-performance pressure sensing

Na Zheng[1, 2], Changzhou Chen[1, 2*], Mengqi Tang[1, 2], Weixin Wu[1, 2], Yan Jiang [1, 2] Douyong Min[1,2]

Optimization of PDMS concentration

PDMS and N-hexane mixed solvent with different concentration of PDMS was prepared by adding PDMS base agent (0.5 g, 1.0 g, 1.5 g and 2.0 g) and curing agent (base agent and curing agent in a mass ratio of 10:1) into 10 mL N-hexane. The detailed preparation of M-SPF samples has been described in section 2.3 and the corresponding products were named as M-SPF-0.5, M-SPF-1.0, M-SPF-1.5 and M-SPF-2.0. We found that the M-SPF-0.5 was fragile and non-elastic, which is not available for flexible sensing material. The densities of M-SPF-1.0, M-SPF-1.5 and M-SPF-2.0 were calculated to be 0.358 g/cm^3, 0.571 g/cm^3, 0.726 g/cm^3, respectively, suggesting the thickness of PDMS layer on C-SPF increased as the concentration of PDMS increased. Due to the PDMS is a non-conductive medium, the conductivity of M-SPF will decrease with the increased amount of PDMS. The conductivities of M-SPF-1.0, M-SPF-1.5 and M-SPF-2.0 samples were tested to be 1.47 s/m, 0.61 s/m and 0.19 s/m, respectively. Thus, M-SPF-1.0 with the best conductivity was used as the pressure sensing material in this study.

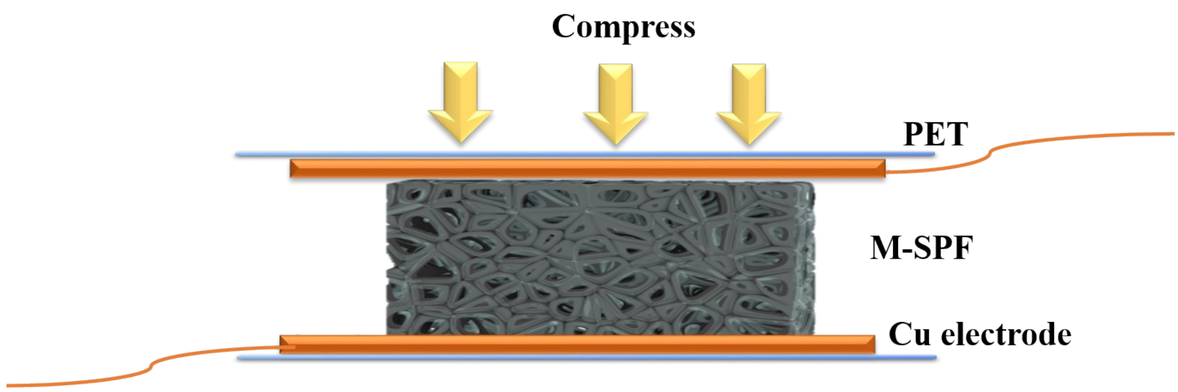

Fig. S1. The composition of the prepared pressure sensor.

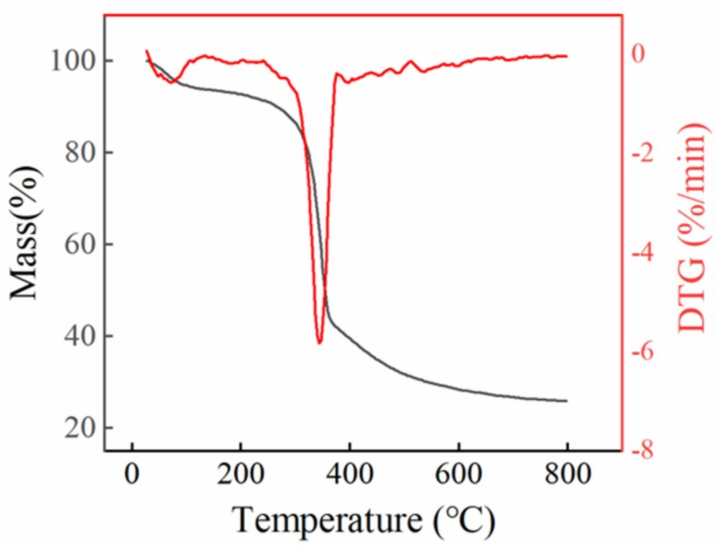

Fig. S2. TG-DTG curves of SPF.

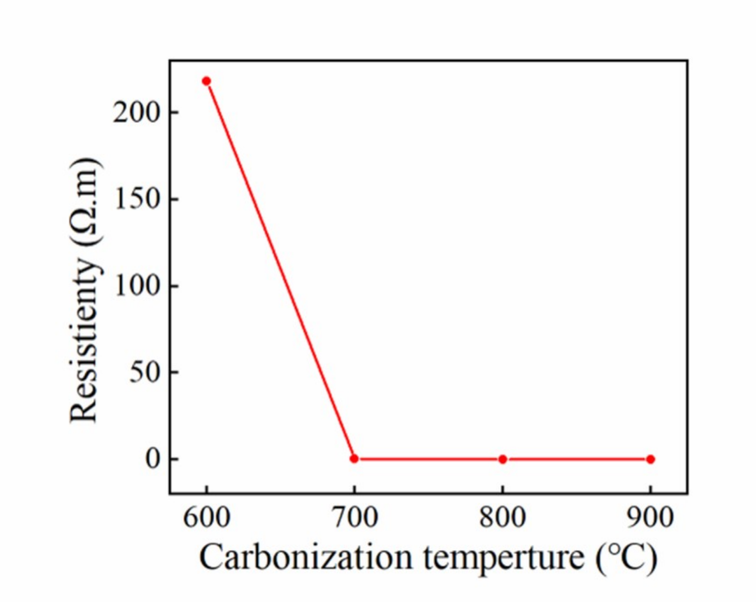

Fig. S3. The conductivity of C-SPFs obtained at different temperatures.

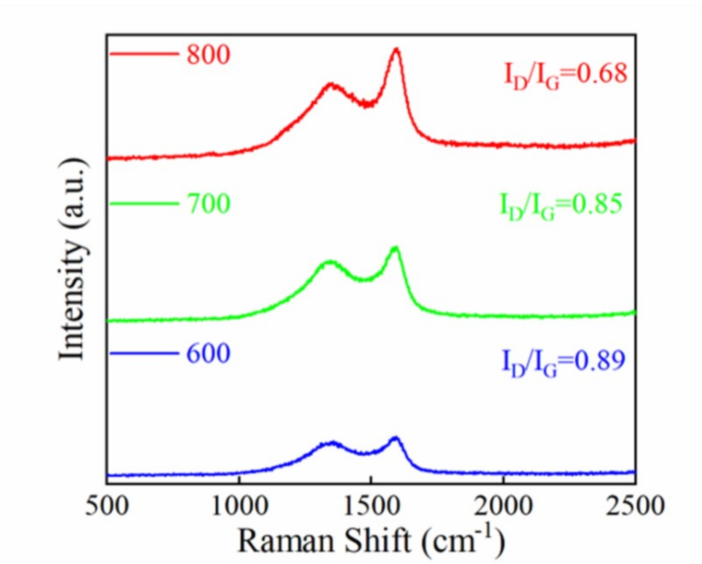

Fig. S4. Raman spectra of samples at different temperatures.

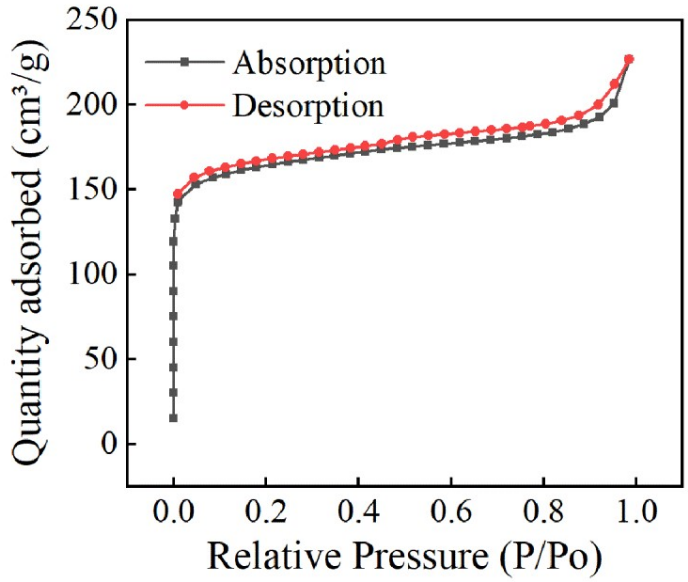

Fig. S5. The nitrogen adsorption and desorption isotherms of C-SPF in Brunauer-Emmett-Teller (BET) measurement.

Fig. S6. Photos of C-SPF before and after compression.

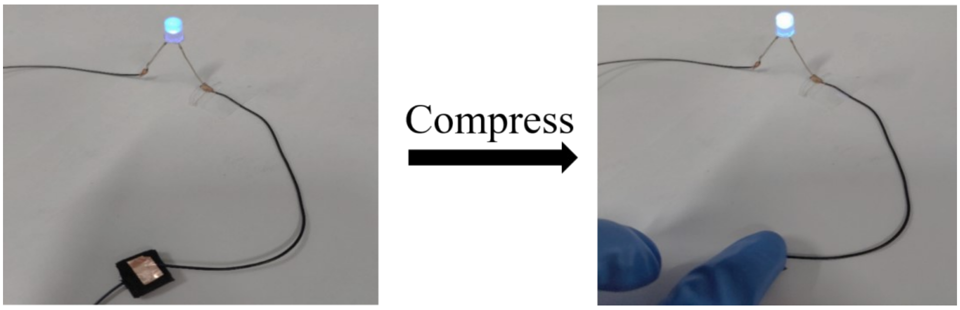

Fig. S7. Changes in brightness of LED lights without pressing and pressing.

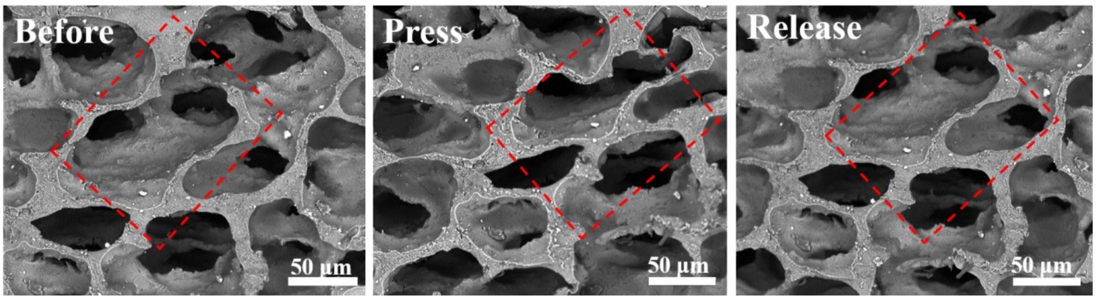

Fig. S8. SEM images of M-SPF in the process of compression and release.

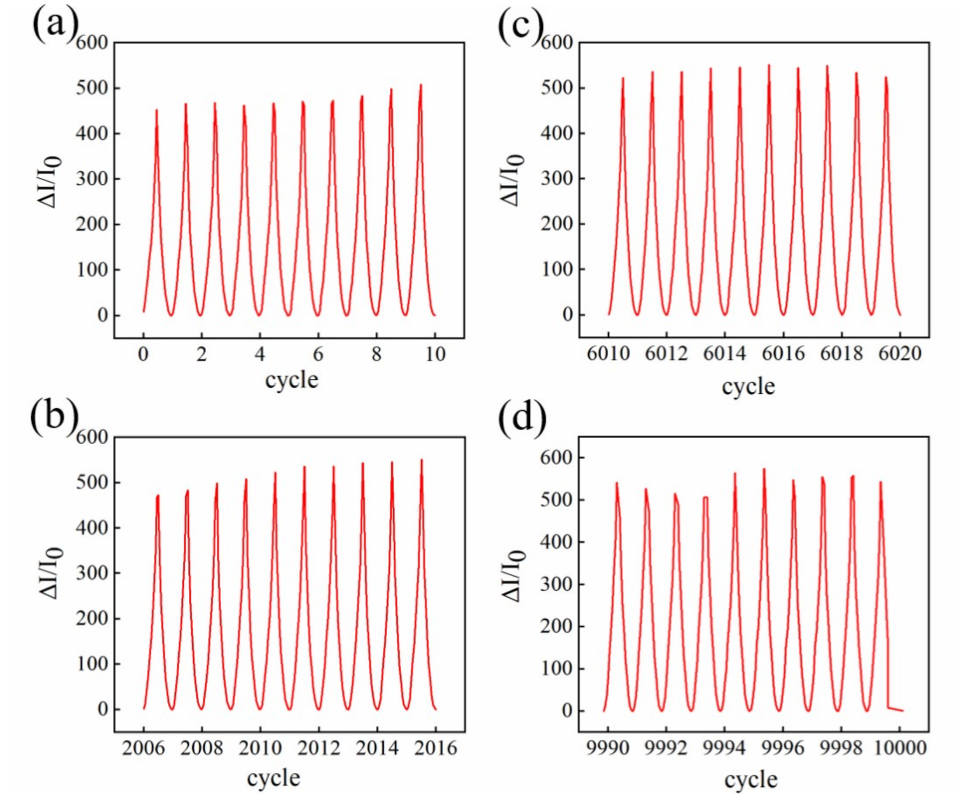

Fig. S9. Partial electrical response curves for 10,000 cyclic of M-SPF at 50% strain.

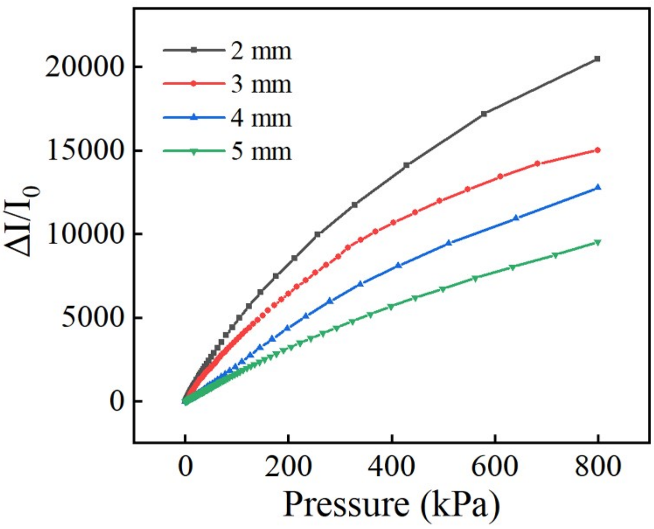

Fig. S10. The effect of thickness on the sensitivity of M-SPF-based sensor.

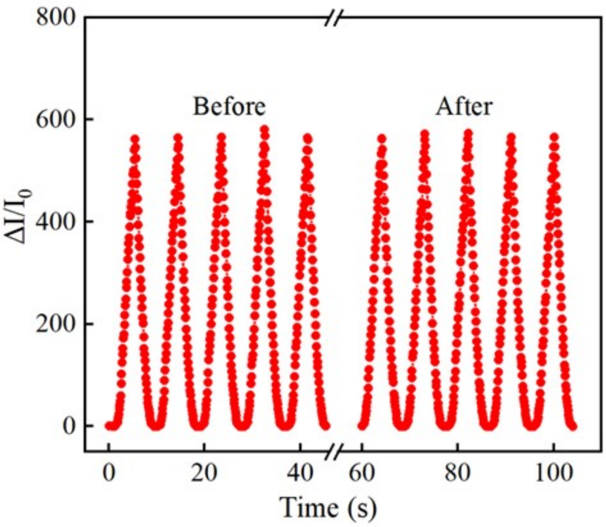

Fig. S11. Response of the same pressure sensor to electrical signals at 50% strain before and after three months.

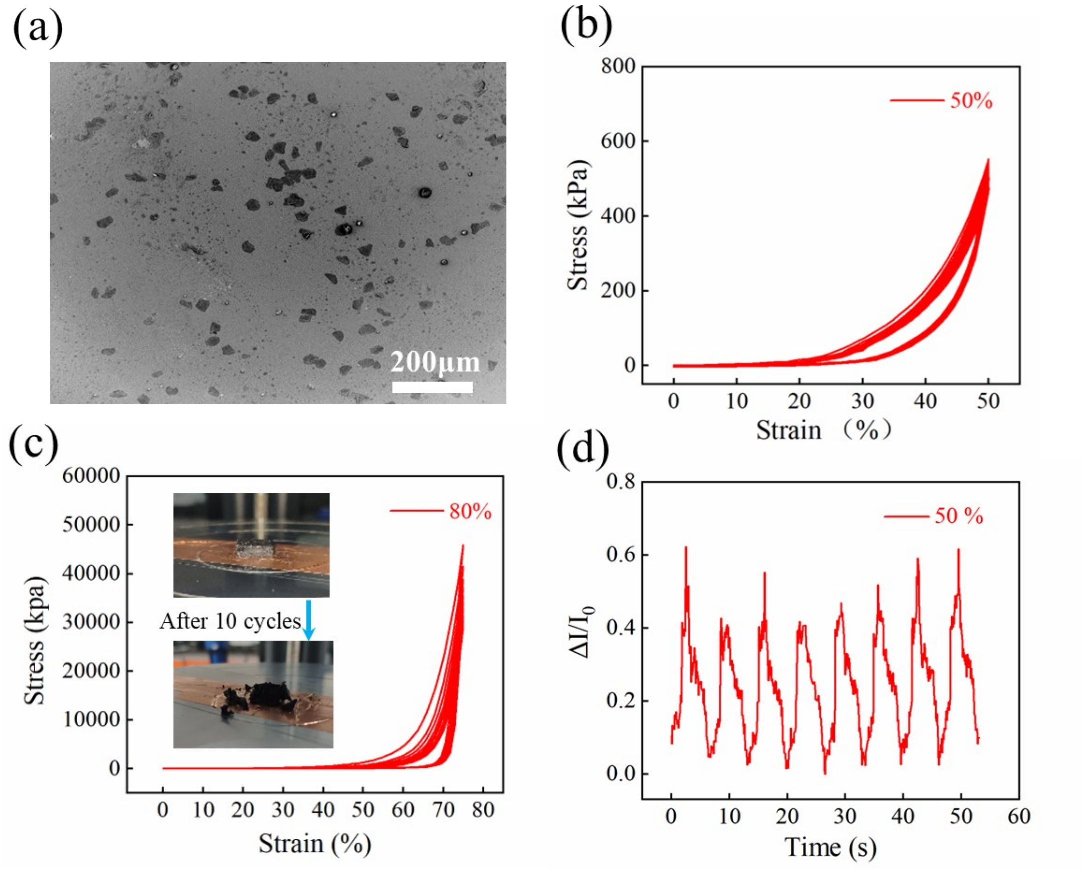

Fig. S12. (a) SEM image of CSPP-PDMS (b) 100 cyclic loading–unloading curves under 50% compression strain. (c) 10 cyclic loading–unloading curves under 80% compression strain. (The inset represents the appearance of CSPP-PDMS before and after compression) (d) The RCR of the CSPP-PDMS based pressure sensor under 50% strain.

Table S1 The bulk density, porosity and the ratio of carbon and oxygen content of the samples.

Samples	Bulk density (g/cm^3)	Porosity (%)	C/O
SP	0.0841	89	2.10
SPF	0.0342	94	2.53
C-SPF	0.0257	93	9.59
M-SPF	0.3584	67	1.76

Table S2 Material properties of each component in the simulation work.

Samples	Bulk density (g/cm^3)	Elastic modules(kPa)	Poisson ratio
C-SPF	0.0257	0.65	0.25
M-SPF	0.3584	21.9	0.35

Table S3 Comparison of the detection range and sensitivity for various pressure sensing materials.

Materials	Detection range and Sensitivity	Ref.
2D WSe_2 Nanosheets	1 -100 kPa (S=29.24 kPa^{-1})	14
2D $MoSe_2$ Nanosheets	0.001-0.5 kPa (S=18.42 kPa^{-1}) 1-35 kPa (S=7.28 kPa^{-1}) 40-100 kPa (S=2.63 kPa^{-1})	15
Alginate and graphene Sponge	5 kPa (S=5 kPa^{-1}) 50 kPa (S=1 kPa^{-1}) 500-1000 kPa (S=0.005 kPa^{-1})	17
rGO and Polyaniline Sponge	0-27 kPa (S=0.152 kPa^{-1})	19
PANI Paper	2-90 kPa (S=2.23 kPa^{-1})	20
PPy and Cotton	0.1-5 kPa (S=4.5 kPa^{-1})	21
Graphene–Polyurethane Sponge	0-2 kPa (S=0.26 kPa^{-1}) 2-10 kPa (S=0.03 kPa^{-1})	50
GO- Hybridized CNTs Aerogels	0-1 kPa (S=1.22 kPa^{-1}) 1-8 kPa (S=0.39 kPa^{-1})	51
Silver Nano-flower Decorated Graphene Oxide-Sponges	0-10 kPa (S=0.572 kPa^{-1})	52
Carbon Black and Polyurethane Sponge	0-2 kPa (S=0.068 kPa^{-1}) 2-10 kPa (S=0.023 kPa^{-1}) 10-16 kPa (S=0.036 kPa^{-1})	53
Nano-fibrous Aerogels	0-3.5 kPa (S=0.43 kPa^{-1}) 3.5-5 kPa (S=1.02 kPa^{-1})	62
CNT/rGO–CNF carbon aerogel	0-0.1 kPa (S=22.05 kPa^{-1}) 0.1-1 kPa (S=11.82 kPa^{-1}) 1-5 kPa (S=0.44 kPa^{-1})	64
Carbide Nano-sheets and Bacterial Cellulose Carbon Aerogels	0-10 kPa (S=12.5 kPa^{-1})	S1

Aligned carbon nanotubes/graphene	0-0.3 kPa (S=19.8 kPa^{-1}) 0.3-6 kPa (S=0.27 kPa^{-1})	S2
Graphene Sponges	0.3-10 kPa (S=0.046 kPa^{-1}) 10-40 kPa (S=0.007 kPa^{-1})	S3
Graphene/Polyimide Nanocomposite Foam	0-1.5 kPa (S=0.18 kPa^{-1}) 1.5-7 kPa (S=0.023 kPa^{-1})	S4
M-SPF	1-10 kPa (S=48.5 kPa^{-1}) 10-100 kPa (S=63.4 kPa^{-1}) 100-800 kPa (25.6 kPa^{-1})	This work

References

S1. Z. Chen, Y. Hu, H. Zhuo, L. Liu, S. Jing, L. Zhong, X. Peng and R. C. Sun, *Chem. Mater.*, 2019, **31**, 3301-3312.

S2. M. Jian, K. Xia, Q. Wang, Z. Yin, H. Wang, C. Wang, H. Xie, M. Zhang and Y. Zhang, *Adv. Funct. Mater.*, 2017, **27**, 1606066.

S3. L. Zhu, Y. Wang, D. Mei and X. Wu, J. Microelectromech. S., 2019, **28**, 154-163.

S4. Y. Qin, Q. Peng, Y. Ding, Z. Lin, C. Wang, Y. Li, J. Li, Y. Yuan, X. He and Y. Li, ACS Nano, 2015, **9**, 8933-8941.